Surface Curvature Effects in Physisorption and Catalysis by Microporous Solids and Molecular Sieves

ERIC G. DEROUANE,[*,1] JEAN-MARIE ANDRE,[*] AND AMAND A. LUCAS[†,2]

Facultés Universitaires N.D. de la Paix, Centre de Recherche sur les Matériaux Avancés, Rue de Bruxelles 61, B-5000 Namur, Belgium; and †IBM Almaden Research Center, San Jose, California 95120

Molecular sieves, including zeolites, distinguish themselves from other sorbents and catalysts by the curvature of the surface (internal pores and cages, and external "pockets") which they offer to incoming molecules on their way to catalytically active sites. Elaborating on the recently proposed general concept of "nesting," this paper attempts to quantify one of its aspects, namely the role of surface curvature when the size of the host structure and that of the guest molecule become comparable. Topics and examples are selected from the literature on physisorption and/or catalysis by zeolites. A simple van der Waals model for the interaction energy and the sticking force of a molecule lodging in a pore is used to rationalize semiquantitatively a number of well-accepted observations, e.g., (i) the role of zeolites as molecular traps; (ii) the origin of the surface barrier postulated to reconcile the large divergence between intracrystalline (self-diffusion) and macroscopically measured (nonequilibrium) diffusion coefficients; (iii) the rapid diffusion of molecules in tight-fitting zeolite pores; (iv) the "window effect" observed for the diffusion of C_3–C_{14} linear chain paraffins in erionite; (v) the relationship among apparent acid strength, cracking activity, and molecular "nesting"; and (vi) the dependence of the "constraint index" on temperature. In particular, two new concepts are introduced: the *floating* molecule which acquires supermobility when its dimension(s) matches closely that of the surrounding channel and the serpentine or *creeping* motion of the molecule along the channel walls. © 1988 Academic Press, Inc.

INTRODUCTION

In studying molecular sieves, among which are many zeolites, as sorbents or catalysts at the atomic level, it occurred to us that the geometric curvature of their surfaces (internal pores and cages, external "pockets") accessible to incoming molecules may have consequences for the physical state of the system and influence the chemical evolution of the sorbed molecules. Such curvature effects have not always received the necessary attention since interest has been focused primarily on other remarkable qualities of the catalytically active sites offered by these microporous materials (*1*).

We recently proposed the idea, and coined it the "nest effect" (*2*), that molecules and their direct curved framework environment in zeolites tend to reciprocally optimize their van der Waals interaction. Electronic perturbations and thus conformational changes may result therefrom for the sorbed species as well as, if allowed, for the sorbent framework. The latter effect is probably exemplified by the changes occurring upon sorption of various molecules by zeolite ZSM-5, as observed by NMR and X-ray diffraction spectroscopies (*3*). This view is related to the "supermolecule" concept, that is a unique system where individual molecular components are interacting noncovalently and harmonize their respective geometry and conformation, familiar to the theoretical chemist (*4*) and of broad application in enzymatic catalysis.

Laplace (*5*) and Kelvin (*6*) were the first to account on a general basis for the effect

[1] To whom correspondence should be addressed.
[2] Permanent address: Institut de Recherche sur les Interfaces Solides, Rue de Bruxelles 61, B-5000 Namur, Belgium.

of surface curvature on interfacial energy. However, their approach is not applicable to pores of molecular size, i.e., of diameter below about 2 nm (7). Gas phase diffusivities for linear hydrocarbons in shape-selective zeolite ZSM-5, exceeding by one to two orders of magnitude those expected from Knudsen diffusion, have been evaluated: this observation is at the origin of the configurational diffusion concept (8). The role played by the fit between the molecules and the channels is thereby recognized and the Knudsen diffusion model must be entirely abandoned. Its assumption of random (no memory) angular rebounding (fully inelastic collision) for each molecule–wall encounter does not hold for such systems in which momentum vectors will have preferential orientations due to the comparable sizes of the molecules and channels. Molecules thus behave as a one-dimensional gas in van der Waals interaction with the pore walls, a state not unlike that called "supermobile" by Kemball (9).

Elaborating on the above nest effect for sorbed molecules accommodated in molecular sieves or zeolites, we attempt in this paper to quantify further the role of surface curvature, to extend previous concepts considering the influence of micropore geometry on sorbed molecules, and to delineate principles applicable to a variety of isolated observations and results for which there exists a need for quantification and coherent description.

METHOD

Model for the van der Waals Interaction of a Molecule with a Curved Surface

The essential problem being the appreciation of the effects of the tridimensional confinement of zeolite pores on the guest molecules, concave pore geometries only will be considered. The simplified approach described below is currently being refined to remedy the assumptions of the model which so far is justified mainly by its semiquantitative applicability and implications.

The salient points of the model and further possible refinements will be reported and discussed elsewhere (10).

As a very first approximation, the zeolite is represented as an isotropic dielectric continuum with dielectric constant $\varepsilon(\omega)$. The case of a molecule with isotropic polarizability in a spherical or cylindrical pore has been discussed in earlier papers (11–13). The type of effect for which we are searching evidence is revealed by considering the simplified interaction of a point isotropic molecule of dynamic scalar polarizability $\alpha(\omega)$ with a perfect metal ($\varepsilon = \infty$) environment. Equation [47] of Ref. (11) yields as van der Waals energy W,

$$W(r) = -(C/D^3) \sum_{n=1}^{\infty} n(n + 1)r^{2n+1}, \quad (1)$$

where $r = D/a$ is the ratio of the distance of the molecule from the center of the cavity to the radius of the latter (Fig. 1) and C is a molecular constant given by

$$C = (h/2\pi) \int_0^{\infty} \alpha(i\omega) \, d\omega. \quad (2)$$

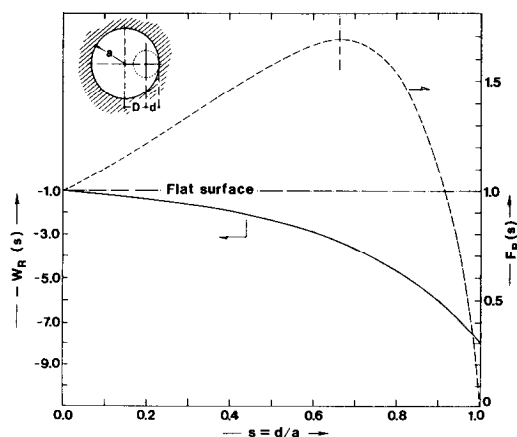The summation in Eq. (1) can be expressed as a geometrical series and yields

FIG. 1. Variation of $-W_r(s) = -W(s)/W(0)$ and $F_r(s) = F(s)/F(0)$ as a function of $s = d/a$ in the interval $0 \leq s \leq 1$, i.e., as a function of the cavity (pore) size a for a fixed sorption distance (molecular size, assuming van der Waals contact) d and vice versa.

$$W(r) = 2(C/D^3)r^3(r^2 - 1)^{-3}. \qquad (3)$$

The van der Waals attraction force toward the pore wall is thus

$$F(r) = -\partial W/\partial D$$
$$= 12(C/a^4)r(r^2 - 1)^{-4}. \qquad (4)$$

Setting $s = 1 - r = (a - D)/a = d/a$, with d the distance from the point molecule to the pore wall (Fig. 1), Eqs. (3) and (4) become

$$W(s) = -(C/4d^3)(1 - s/2)^{-3} \qquad (5a)$$

and

$$F(s) = (3C/4d^4)(1 - s)(1 - s/2)^{-4}. \qquad (5b)$$

The first factors in the expressions of $W(s)$ and $F(s)$ are the van der Waals energy and force, respectively, for a flat surface ($a = \infty$ or $s = 0$) and a sorption distance d, whereas the other factors bring the corrections due to the curvature of the surface. Setting the values $W(0)$ and $F(0)$ for the flat surface, the ratios

$$W_r(s) = W(s)/W(0) = (1 - s/2)^{-3} \qquad (5c)$$

and

$$F_r(s) = F(s)/F(0)$$
$$= (1 - s)(1 - s/2)^{-4} \qquad (5d)$$

are easily calculated. They are plotted in Fig. 1 as a function of $s = d/a$ in the interval $0 \leq s \leq 1$, i.e., for a fixed sorption distance d as a function of the cavity (pore) radius a, and vice versa.

The advantage of considering the simple case of a "metallic" substrate is apparent in the above result: there is, for this case, factorization of the intrinsic molecular property (dipole polarizability) and the extrinsic geometrical curvature effect of the substrate. In a more realistic treatment of the substrate dielectric response (*11*), such a factorization does not take place so that the role of spatial confinement is not easily disentangled from the molecular properties. However, we are confident that these simple "metallic" formulas will remain qualitatively valid as scaling rules for the geometrical confinement effect.

It is seen from these equations that:

(i) The relative van der Waals attractive energy $W_r(s)$ increases monotonically when the pore size decreases and eventually reaches several times the value of the flat surface ($s = 0$) when the pore radius equals the sorption distance ($a = d$, $s = 1$). The increase in sorption energy with surface curvature can be interpreted as a focusing effect of the concave surface for the virtual quanta of collective excitations exchanged between the sorbate and its environment.

(ii) The relative van der Waals force $F_r(s)$ reaches a maximum for $a = 1.5d$ ($s = \frac{2}{3}$) and decreases rapidly toward zero for $d > 0.9a$ ($s > 0.9$), i.e., when the fit of the molecule within the pore becomes tight. When the optimal fit is reached, $a = d$ ($s = 1$), the sticking force $F_r(s)$ vanishes and the *molecule* appears as *floating* in the pore, which is the ideal situation to achieve supermobility (*9*). Clearly, the van der Waals force is canceled by an equal and opposite force from the pore wall when the molecule is at the *equilibrium* adsorption distance. However, for any other molecule–substrate separation larger than the equilibrium value, the van der Waals force is by far the dominant one and is the one which causes sticking. Its weakening value for tighter fit is what we suggest could entail supermobility, and if repulsion is taken into account it is relevant to note that $F_r(s)$ will go in fact to zero before tight fitting ($s = 1$) is reached (*10*).

If a cylindrical pore is considered, we will in the discussion below apply Eqs. (5a)–(5d) as a first approximation, assuming that $a = (1.5)^{1/3}r_p = 1.145r_p$, r_p being the crystallographic radius of the pore. The correction coefficient is determined by comparing the relative volumes of a sphere ($a = r_p$) and a cylinder (radius $= r_p$ and length $= 2r_p$) possessing identical curvatures.

The variations of $W_r(s)$ and $F_r(s)$ can be visualized further by considering the qualitative schemes of Fig. 2 representing
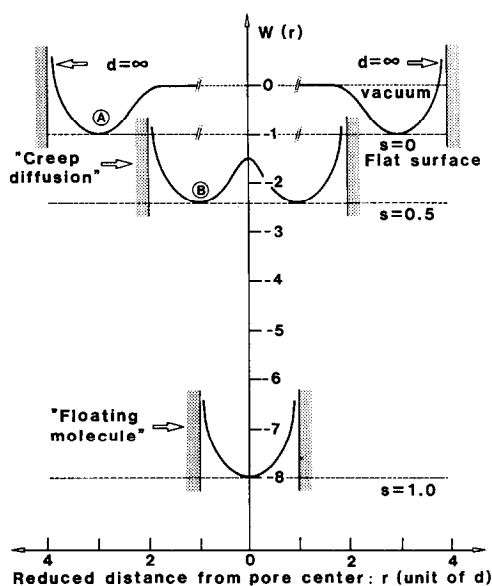
FIG. 2. Schematic representation of the van der Waals attraction potential $W(r)$ as a function of the reduced distance from the pore center (units of d). Repulsion effects are introduced qualitatively.

changes in the van der Waals attraction potential well as a function of the reduced distance from the pore center (units of d). For the sake of clarity, repulsion effects have been qualitatively represented at short distances to the pore wall. It is then concluded that:

(i) a given molecule (d fixed) will try to reach sorption positions with the smallest allowed value of a ($a \geq d$);

(ii) the center of the pore never corresponds to an equilibrium and stable position unless $s = 1$, that is when the pore and the sorbed molecule have similar van der Waals dimensions (case of the ideally "floating" molecule, $a = d$);

(iii) given the large increase in sorption energy as compared to the flat surface case, we are then led to envisage molecular displacement in the pores at not too high temperatures as a crawling motion effected by local deformations of molecular segments, of vibration, rotation, or libration types, while the whole molecule sticks to or "wets" the pore wall. Therefore, the trans-

lation of molecules in zeolite channels appears, at moderate temperature, as a creeping locomotion along the zeolite walls, which we will refer to as "creep" diffusion or motion.

The latter conclusion necessitates two remarks: first, the creep model of diffusion does not apply to spherical molecules or atoms (CH_4, Xe, . . .) which probably hop as a whole over the corrugation barriers of the wall, and second, the whole chain of a molecule will have a finite probability to be lifted and to slide or dangle all across the pore at temperatures $T > |W(s)|/k$.

Finally, it must be emphasized that the two basic ideas quantified in this model,

(i) $|W(\text{concave surface})| > |W(\text{flat surface})| > |W(\text{convex surface})|$, and

(ii) F (concave surface) going to zero for tight fitting,

also hold true for any kind of pairwise additive interactions between molecules. In particular, they are not restricted to van der Waals interactions but also hold for Madelung or Debye type interactions which apply to polar materials. In the latter case, however, the geometrical factor describing the curvature effect ($s = d/a$ dependence) will be different.

RESULTS AND DISCUSSION

The main objective of the treatment below is to test the conceptual validity of the aforementioned model on the basis of reliable results selected from the available literature. The importance of physisorption in catalytic transformations should stand whenever active sites are located in a curved environment, e.g., in the intracrystalline volume of zeolites or on their hilly external surface (2).

Physical consequences of surface curvature will be dealt with first. As an example, noncovalent molecule-zeolite interactions (physisorption) could well be at the origin of sorbate-induced framework structural changes, for example, those observed by X-

TABLE 1

Size Parameters for Certain Zeolites and Molecules

Pore sizes of selected zeolites		
Zeolite type	Pore size $(2r_p, \text{Å})^a$	Effective pore size $(2a, \text{Å})$
ERI (Erionite): window	4.47 (C)	5.12
cage	6.30 (C)	7.21
MEL (ZSM-11)	5.30 (C)	6.07
MFI (ZSM-5)	5.40 (C)	6.18
MOR (Mordenite)	6.85 (C)	7.84
LTL (L,...)^b	9.00 (S)	9.00 (S) or 10.3 (C)
FAU (X, Y,...)	11.80 (S)	11.80

Critical molecular sizes^c		
Molecule	Critical diameter $(2r_m, \text{Å})$	Length (Å)
Ne	3.20	—
Ar	3.83	—
Kr	3.94	—
Xe	4.37	—
Methane	4.44	—
Ethane	4.60	5.26
Propane	4.60	6.52
Linear alkanes (C$_n$)	4.60	$5.26 + 1.26 (n - 2)$

^{a} Average quadratic value of the pore radius derived from the actual channel dimensions listed in Ref. (21). (S) and (C) refer to spherical (cavity) and cylindrical pores, respectively. The last column lists the effective pore diameter $2a$ with $a = r_p$ for spherical pores and 1.1447 r_p for cylindrical pores, see text.

^{b} Considering that zeolite L is built of nearly spherical cavities of about 9 Å connected via 7.1-Å windows.

^{c} Values selected from Refs. (19, 20), based on Pauling's values of bond lengths and van der Waals radii of atoms.

ray diffraction and nuclear magnetic resonance (NMR) spectroscopies upon sorption of various organic molecules on zeolite ZSM-5 (3, 14). Then, we will emphasize the important role that (physi)sorption equilibria can sometimes have on reaction kinetics. These do influence the local (internal) concentration of the chemical species (reactants, intermediates, products) near the active sites which are involved, and thus the rate of reaction, as already pointed out in some cases (2, 15–18). Note also that the high heats of physisorption expected as a result of surface curvature effects may eventually exceed the activation energy of many chemical reactions, a point previously made by Barrer (19).

Table 1 lists the pore and molecular size parameters (19–21) which will be used throughout the following evaluation for our approach. Whenever possible, use of data for high Si/Al ratio materials will be preferred in order to minimize contributions from variations in aluminosilicate framework polarizability, polarity, and channel constraints induced by exchange cations, the importance of these factors increasing with structural Al content. In addition, systems will be selected in which repulsion effects, not taken specifically into account by the model, should be small. When dealing with catalytic reactions, it must be recognized that the surface curvature effects operate along the whole reaction pathway.

PHYSICAL CONSEQUENCES OF SURFACE CURVATURE EFFECTS

Physisorption and Molecular Trapping

The ability of molecular sieves to trap molecules which can access their intracrystalline void volume is one of their earliest and most demonstrated properties.

When considering the isosteric heat (Q_S) or the differential heat ($-\Delta H \approx Q_S$) of sorption of a variety of molecules on microporous sieves, two striking observations usually emerge:

–the initial (extrapolated to zero coverage) adsorption heat rises rapidly when the molecule size becomes comparable to the pore size for a given molecule sorbed by zeolites or other adsorbents with different channel openings (22).

–initial Q_S values tend to decrease rapidly with coverage, eventually reaching a plateau, for small molecules while, for larger sorbates, heats of sorption are approximately constant (23).

The above observations are easily and immediately rationalized by consideration of Eqs. (5a)–(5c) and Figs. 1 and 2.

Clearly, adsorption heats should increase monotonically as the value of $s = d/a$ tends progressively to unity, e.g., when the pore radius a decreases and becomes eventually equal to the van der Waals radius d of the

molecule. Equation (5c) enables one to calculate $W_r(s)$ values from which relative sorption energies are easily derived for a given molecule interacting with sorbents of varying pore size. The reverse situation, one given structure and different molecules, cannot be treated simply by consideration of Eqs. (5) as the guest molecule polarizability which has an important effect on sorption heat must also be considered (19). Thus, the validity of our model is easily tested by comparing, for example, the experimental and calculated sorption heats of methane on various zeolites, as is done in Table 2. Calculated values, $Q_S(i)$, are evaluated relative to the heat of sorption of methane on zeolite Y (FAU structure type), $Q_S(FAU)$ being taken as reference, using the equation

$$Q_S(i) = Q_S(FAU) \cdot [W_r(s_i)/W_r(s_{FAU})] \quad (6)$$

in which $W_r(s_i)$ and $W_r(s_{FAU})$ are $W_r(s)$ values for zeolites i and FAU, respectively. The strikingly good agreement that is observed originates in part from the "spherical" conformation of the methane molecule.

In the limiting case of a close fit between the adsorbate and a spherical pore, it is worth pointing out that the present model agrees with half-a-century-old dispersion energy calculations (26) predicting that

sorption heats for this situation can be as much as eight times larger than the planar surface value. If a hemispherical pore on a surface or the bottom of a cylindrical pore is considered, the multiplication factors are reduced to 4.00 and 6.36, respectively. Related pertinent literature has been reviewed by Barrer (60). Note that such situations may apply to pockets likely to be found on the external hilly surface of zeolite crystals or those present in zeolite channels, e.g., mordenite, of which the essential features can be derived from the zeolite crystallographic structure.

One can also conclude from such considerations that sorbed molecules will first achieve the best possible fit between their size (and shape) and that of the intracrystalline environment in order to maximize their van der Waals attraction energy. For small molecules, higher "zero coverage" (initial) sorption heats will thus be observed as those will be accommodated first in the smallest pores (rings, prisms, side pockets, channels) where optimal match is achieved, and the sorption heat will rapidly decrease to a plateau for higher coverages. This phenomenon explains the apparent physical site heterogeneity observed in the initial stages of their physisorption. For large and bulky molecules, such a situation occurs only to a very limited extent, which explains the notable absence of this phenomenon in that case.

Consequently, we propose that the molecular trapping effect of zeolites and other molecular sieves is directly related to the increase in physisorption energy resulting from their high surface curvature. This energy is much larger than its thermal counterpart. Thus, the sorption equilibrium is strongly displaced toward adsorption at room temperature or below and physical desorption occurs usually only to a noticeable extent at temperatures higher than ambient. Note also that for such highly curved surfaces, the term "surface area" loses its significance as the sorbate molecules interact with their whole environment. Sorption

TABLE 2

Heats of Sorption (Q_s) of Methane on Zeolites

Zeolite	Experimental value (kJ mol⁻¹)	Calculated value (kJ mol⁻¹)[a]	Reference
FAU	15.2	(15.2)	24
LTL	18.0–20.0	19.2	19
MOR	23.0	22.5	See[b]
ZSM-5	28.0	32.0	25

[a] Relative to the sorption heat of methane on zeolite Y taken as reference. Calculated according to the model (Eq. (5a)). See Table 1 for methane and pore sizes.

[b] Evaluated from Fig. 11 in Ref. (19).

capacities should be expressed preferably in terms of sorbed volumes or weight unless one favors the use of a "monolayer equivalent area," which needs to be carefully defined. This remark applies to numerous past and current reports in both the journal and the patent literatures.

External Surface Barrier to Sorption

To explain the four to six orders of magnitude difference between measured uptake (D_{uptake}, from sorbed volume or weight) and self-diffusion coefficients (D_{NMR}, from NMR relaxation data) for intracrystalline molecular diffusion, the existence of a transport resistance, i.e., a surface barrier, at the external surface of zeolites was postulated (20, 27). Models which assume either the blockage of a majority of pores at the external surface of the crystallites (by amorphous deposits) or a reduced diffusivity in a surface layer, owing to structural changes (28), have been proposed.

Not excluding the possible occurrence of such causes, another general explanation may be proposed by consideration of the principles illustrated in Figs. 1 and 2. Molecular transferral from the gas into the restricted zeolite channels is unlikely to occur by direct impingement because the molecules, unless they are mono- or maybe diatomic, will not have the proper orientation and/or configuration relative to the pores. Therefore, their initial physisorption state is likely to be on the zeolite external surface, e.g., state A in Fig. 2, where the entropy decrease due to adsorption will take place. The next step consists in diffusion into the intracrystalline void volume, e.g., going from state A to state B by moving over the rim of the pore, which requires an activation energy not larger than the physisorption heat on the external surface (if transport is via the gas phase) or one-half the latter if surface diffusion is involved (29). A sketch of the physisorption energy experienced by a molecule is shown in Fig. 3, as it moves at constant distance from the surface across a pore opening (the pore is
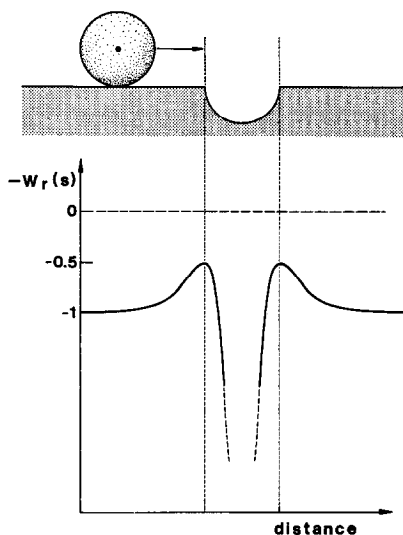

FIG. 3. A sketch of the inhomogeneous physisorption energy $W_r(s)$ on a flat surface with a crater for a constant molecule–surface distance.

shown as a hemispherical crater in the flat surface). Note that the origin of the barrier for entering the pore is the convex curvature of its rim which reduces the adsorption energy as compared to the flat surface value. If the activation energy shown around the pore rim is at the origin of the surface diffusion barrier, (D_{NMR}/D_{uptake}) factors of 6.10^3–4.10^7 at 273 K are explained readily, considering that the above heat values should be in the vicinity of 20–40 kJ mol^{-1}.

This proposal holds if intracrystalline molecular motion is rapid. Note also that the existence of such surface barriers should affect the temperature at which uptake occurs and thus play a role in the molecular sieving of mixtures of simple mono- or diatomic species. Hints for the existence of such effects have been given by Barrer (19, 30).

Sorption and Diffusion

The effect of surface curvature on sorption heats, as discussed above for methane, applies to all molecules. The following discussion will however be restricted to the

case of alkanes to emphasize the variables that are most likely to have catalytic implications.

Initial heats of sorption of linear alkanes ($2 \leq n_C \leq 6$) are found to increase linearly with carbon number (n_C) for various zeolites, among which as examples are the structure types MFI (22), FAU (22), and LTL (31) shown in Fig. 4. The following equations giving the dependence of Q_S (kJ mol^{-1}) on n_C are approximately obeyed,

$$Q_S(\text{MFI}) = 15n(\text{CH}_3) + 9.7m(\text{CH}_2) \quad (7a)$$

$$Q_S(\text{LTL}) = 13.6n(\text{CH}_3)$$
$$+ 8.4m(\text{CH}_2) \quad (7b)$$

$$Q_S(\text{FAU}) = 11n(\text{CH}_3) + 7.0m(\text{CH}_2), \quad (7c)$$

$n(\text{CH}_3)$ and $m(\text{CH}_2)$ being the number of methyl and methylene groups, respectively.

These relations indicate that a methyl group contributes more to the sorption heat relative to a methylene group and that these two contributions are additive and increase when the pore size decreases, i.e., when $s = d/a$ becomes larger. Considering the size of the CH$_3$ and CH$_2$ groups, about 3.5 Å in diameter, their relative sorption heats (FAU used as reference) for various pore dimensions are calculated according to Eq. (5c) to be 1, 1.17, and 1.67 for the FAU, LTL, and MFI structure types, respectively. These values agree qualitatively with those derived from the above experimental variations, i.e., 1, 1.20, and 1.37 in the same order.

In addition to providing further support for our model, this analysis indicates that the alkane–zeolite interaction is the sum of molecular segment–zeolite contributions, where the segments are either terminal CH$_3$ or chain CH$_2$ groups. This scheme fits the general picture of van der Waals interactions in their pairwise additive property. The smaller contribution of CH$_2$ is related to its smaller polarizability relative to CH$_3$.

This separation of molecule–zeolite interactions into segmental contributions agrees with the original proposal of Barrer

and Davies (32) on the diffusion mechanism of *n*-alkanes in zeolites (33). The latter was described as a sequence of segmental rotations of only part of the molecule (around a C–C bond), thereby changing the position of its center of mass but not necessarily implying the simultaneous translation of all its parts. This concept is supported by the observation that self-diffusion activation energies for linear alkanes approach an asymptotic limit that is only a rather small fraction of their sorption heat (19, 30).

We propose that molecular displacement in the pores occurs by creep motion and hopping as discussed earlier, the most stable position of the diffusing molecules being off center as indicated in Fig. 2. Note that similar (double-well) profiles were obtained in previous work (34) using a summation of Lennard–Jones potentials to calculate the potential energy of simple molecules in the mordenite and ZSM-5 pores and that energy barriers equal to several kJ mol^{-1} were found to separate one position on the pore wall from its diametrically opposed counterpart. "Jump" times will govern diffusivity in this picture; they should correlate somehow inversely to the sticking force $F(s)$ expressed by Eq. (5b). The average segmental physisorption heat and therefore also the averaged value of $F(s)$ will have to be considered if different parts of the mole-
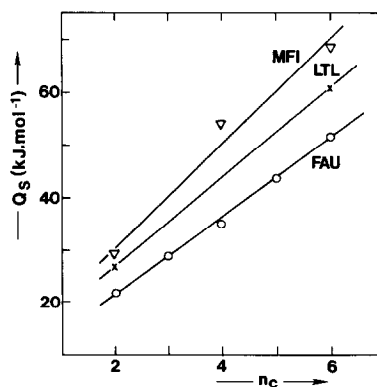

FIG. 4. Initial sorption heats (Q_s, kJ mol^{-1}) as a function of the carbon number n_C of linear alkanes. Zeolite structure types: O, FAU; x, LTL; △, MFI.

cule lie in environments characterized by different s values. This approach will serve as a basis to explain the so-called "window effect" (35, 36) discussed below when evaluating the catalytic implications of surface curvature effects.

Other Properties

In addition to the above considerations, surface curvature effects can also serve as a basis to quantify previous observations. One example is the proposition that higher numbers of bimolecular encounters (37) or molecule-active center collisions (58) are favored in zeolite cavities. Equations (5) support this view by showing quantitatively that the sticking force $F_r(s)$ increases up to $s = d/a = 2/3$ and that the sorption energy $W_r(s)$ can reach up to eight times the ideal flat surface value. Thus, molecules will indeed be concentrated in zeolite pores, i.e., achieve identical coverage at a smaller sorbate pressure in the gas phase relative to a system involving a nearly flat surface ($s = 0$) or large pores ($s \rightarrow 0$), all the other parameters remaining identical. In particular, it is also felt that our model would help in quantifying the chemical NMR shift vs apparent mean free path relationship observed for ^{129}Xe sorbed in various zeolites (38).

Another is the report that two distinct orthorhombic phases are simultaneously formed and coexist when p-xylene is sorbed by monoclinic high Si/Al ratio ZSM-5 crystals (39). The physical nature of this observation is attested by the fact that it does not depend on the chemical nature of the tetrahedral structural sites (other than Si) which constitute the zeolite framework. The form possessing the smallest unit cell volume, attributed to the zeolite containing four ordered xylene molecules per unit cell, is in our scheme the state that favors xylene–zeolite interactions. Indeed, comparing the volume of p-xylene to that of the channel intersections and remembering that the MFI structure possesses four intersections per unit cell, this situation corre-

sponds to one p-xylene molecule per channel intersection. The other form would thus correspond to full loading of the channels by p-xylene and involve also lateral interactions between the p-xylene molecules. The coexistence of both forms implies that their ratio should vary as the amount of sorbed p-xylene tends toward saturation. In both cases, the heat of physisorption could be used to produce local framework distortions (14) near or at structural sites that have lower framework stability (40, 41).

CHEMICAL AND CATALYTIC CONSEQUENCES OF SURFACE CURVATURE EFFECTS

The Window Effect: Diffusion–Kinetics Interaction in Molecular Shape Selectivity

An interesting product distribution was reported for the cracking of n-tricosane (C_{23}-alkane) on erionite, showing maxima for carbon numbers C_{3-4} and C_{11-12} and a very low yield in C_{7-9} products (35). It was rationalized later in terms of "product molecular shape selectivity" on the basis of n-alkane diffusion measurements using the K-form of zeolite T (an intergrowth of offretite and erionite) (36). Indeed, the diffusion coefficients were found to vary in a way similar to that of the product yields; i.e., the preferred product molecules were those possessing high diffusivities. The proposed explanation, coined as the "window effect," was that the less open erionite units acted as bottleneck centers and that a "window of low transmittance" existed for molecules having a critical length comparable to the free length (about 13 Å) of the erionite cage, the latter acting as a low-energy trap. It was thus assumed that alkane molecules of a matching length prefer the cage environment (diameter, 6.3 Å) to that of the smaller pores, and that entropy effects are dominant.

An alternate explanation in energy terms is proposed below on the basis of our model of creep motion, applying the principles of segmental diffusion (see above and Refs.

(*32, 33*)). As translation occurs in this scheme by successive segmental displacements, our approach consists in evaluating the "mean diffusivity" of a segment in alkanes of increasing lengths, of which the various CH_x groups ($x = 2$ or 3) may be affected by different environments. These are the erionite cages which can accommodate a chain of up to eight CH_x segments and the interconnection (window) between those which is able to accept about four CH_x segments. Effective pore sizes for both situations are given in Table 1.

If we assume that diffusivity decreases when the sticking force of the molecule to the zeolite surface increases, we can write as a first approximation

$$D \# \langle F_r(s)^{-1} \rangle \quad \text{or}$$
$$\log_{10} D \# - \log_{10} \langle F_r(s_s) \rangle, \quad (8)$$

where $\langle F_r(s_s) \rangle$ is the average sticking force per segment evaluated as described below.

Each molecular segment i is characterized by a sticking force $F_r(s_{i,j})$ calculated via Eq. (5d), where i denotes the segment and j its environment, i.e., window $j = w$ or cage $j = c$. A critical alkane molecular diameter of 4.6 Å (*20*) is used in all computations; thus, $F_r(s_{i,w}) = 1.106$ and $F_r(s_{i,c}) = 1.683$. In addition, two distinct molecular trapping situations are considered and their probability arbitrarily weighted identically for the sake of simplicity. One maximizes the portion of the molecule lying in the cage, case I (up to eight segments, initially in the cage); in the other situation, case II, the segments occupy initially (up to four) the interconnecting window space between the cages. For each molecule, the following quantities are thus evaluated,

$$F_r(s_j) = \Sigma(i)a_{i,j}F_r(s_{i,j}) \quad \text{with } j = w \text{ or } c, \quad (9)$$

with $F_r(s_c)$ and $F_r(s_w)$ corresponding to case I and case II, respectively. The average sticking forces per molecule $F_r(s_t)$ and segment $\langle F_r(s_s) \rangle$, considering the above definitions and assumptions, are thus given by

$$F_r(s_t) = [F_r(s_w) + F_r(s_c)]/2 \quad (10)$$

$$\langle F_r(s_s) \rangle = F_r(s_t)/n, \quad (11)$$

n being the number of CH_x segments in the molecule under consideration.

Figure 5 shows the plot of $\log_{10} D$ and $-\log_{10} \langle F_r(s_s) \rangle$ vs the carbon number n of n-alkanes in the range C_{3-14}. The positions of the minimum and of the maxima in diffusivity are satisfactorily reproduced. It appears consequently that the essence of the window effect is well accounted for by our model. The discrepancy observed for molecules with carbon numbers 10 to 13 could possibly originate from other molecular conformation effects which are neglected in our approach. On the other hand, although we are confident that the main trends will generally be reproduced by using the aforementioned simple basic model, one should not expect systematic, full, and quantitative agreement in all cases. Indeed, among other factors, Eq. (8) still needs a theoretical basis. Work is progressing in this area.

Nevertheless, in contrast to the earlier proposal (*36*), our explanation attributes principally the observed changes in diffusivity, i.e., the window effect, to a variation in the sticking of the molecules to the pore walls rather than to their ability to reorient rapidly in the cages. Finally, in any case, it
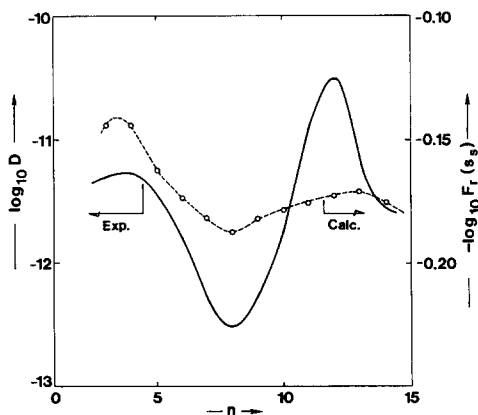

FIG. 5. Rationalization of the window effect. Plot of $\log_{10} D$ (—) and $-\log_{10} \langle F_r(s_s) \rangle$ (---) (see text) vs the number n of carbon atoms for linear alkanes diffusing in zeolite T (OFF-ERI intergrowth) (see also Refs. (*35, 36*)).

is confirmed that the unusual product distribution results from the superposition of a shape-selective pattern of diffusivities onto an intrinsic reaction pattern.

Molecular Nesting vs Acid Strength Effects in Cracking of Alkanes

The following discussion is restricted to zeolite catalysts of which the framework has not been altered during pretreatment and/or subsequent modification(s), including dealumination. In such cases, the number and environment of the acidic sites is well defined and it can be shown that the carboniogenic activity is proportional to the structural Al content (42, 46).

Variations in the acid catalytic activity of zeolites of different Al content and/or structure have been attributed customarily to changes in the acid strength of their Brønsted acid sites resulting from collective effects, considering zeolites as ionic solvents (43) or using intermediate electronegativity concepts (44, 45). These models neglect the contributions of geometrical factors and of physisorption.

Several recent reports indicate that the above interpretation may not hold for materials with Si/Al ratios greater than about 5, in which case two Al structural sites must be separated statistically by more than one Si; i.e., Al sites behave as isolated catalytic entities. Evidence is provided by quantum mechanical calculations evaluating the negative framework charge delocalization in the MFI structure (41); characterizations of Y zeolites with different Al contents (46); ^{1}H magic angle spinning NMR studies of zeolites Y, mordenite, and ZSM-5 (47); and catalytic testing of HY, LaY, and HZSM-5 catalysts (48). The latter study, in particular, supports the nest effect concept (2) by stating that differences can be ascribed to pore structure effects rather than subtle changes in the nature of the active sites.

The nest effect insists, among other things, on the established fact (2, 15–18) that reaction rate constants for intracrystalline zeolite catalysis, to which the funda-

mental principles of catalysis necessarily apply, should be affected by the adsorption equilibria which influence the local (internal) concentrations of the chemical species (reactants, intermediates, transition state complexes) involved along the reaction pathway. Qualitative support was obtained from a volcano-type correlation between turnover frequency (TOF) and pore diameter (2) for a variety of zeolites effecting n-pentane cracking (49). The nest effect is now quantitatively demonstrated below.

The following considerations will hold quantitatively if and when (i) diffusion-disguised kinetics do not operate, (ii) the strength of the Brønsted sites is not altered by the presence of extra framework species, and (iii) the stabilizing surface curvature effect acts along the whole rate-determining step of the reaction pathway, i.e., on the reactants and the reaction intermediates, including the transition state complex or complexes. (Note: the latter is not really an assumption in view of the universal character of the dispersion forces.)

The rate of alkane cracking r_A is given by (50)

$$r_A = k_{HT} \cdot [RH] \qquad (12)$$

in which k_{HT} is the rate constant for hydrogen transfer from alkanes to carbenium ions.

However, as catalysis occurs inside the zeolite pores, one should distinguish between $[RH]_i$ and $[RH]_e$, where the subscripts i and e refer to the intracrystalline and extracrystalline concentrations of the reactant RH, respectively. Thus

$$r_A = k_{HT} \cdot [RH]_i \qquad (13)$$

and

$$r_A = k_{HT} \cdot K_a \cdot [RH]_e \qquad (14)$$

if K_a is the equilibrium constant for the physisorption of RH, accounting for surface curvature effects.

The net rate constant k and the turnover frequency TOF are then given by

$$k = k_{HT} \cdot K_a \qquad (15)$$

$$TOF = k_{HT} \cdot K_a/(Al/(Al + Si)) \quad (16)$$

and it is easily derived that, at constant temperature, turnover frequencies for the conversion of a given reactant by different zeolites are related by the equation

$$\ln(TOF/TOF_r) = \ln R_{TOF}$$
$$= (Q_s(r)/RT) \cdot [(Q_s/Q_s(r)) - 1] \quad (17)$$

as the value of ΔS_a does not depend noticeably on pore size (22). R_{TOF} is the ratio of the turnover frequency, TOF, for a given zeolite to the value TOF_r obtained using a reference material. Q_s and $Q_s(r)$ are the corresponding sorption heats $(-\Delta H_a$ and $-\Delta H_a(r))$, respectively.

This relationship can be used to correlate the data of Ref. (49) obtained for the cracking of n-pentane at 450°C. Medium and large pore zeolites (MFI = ZSM-5, MOR, LTL, and Y) only are considered, for which repulsion effects are likely to be negligible. Highly siliceous ZSM-5 is preferably taken as reference (low Al content, isolated catalytic sites). Thus, $TOF_r = 4.10^{-2}$ (mol (min cat-g)$^{-1}$/[Al/(Al + Si)]) (2, 49) and $Q_s(r) = 59.1$ kJ mol^{-1} (Eq. (7a)) for n-pentane. Q_s and $Q_s(r)$ are related via Eq. (5a) or (5c) and a relationship similar in its form to Eq. (6) for the ratio $Q_s/Q_s(r)$. Equation (17) then becomes

$$\log_{10} TOF = -1.4 + 4.25(R - 1) \quad (18)$$

with

$$R = [a(2a_r - r_m)/a_r(2a - r_m)]^3 \quad (19)$$

and $d = r_m$, i.e., the critical molecular radius, and where the subscript r refers to the reference catalyst, in our case ZSM-5.

Figure 6 shows the correlation between calculated TOF_c and experimental TOF_e turnover frequencies, using the values of Table 1 in Eqs. (18) and (19), and ZSM-5 as reference. The dotted line corresponds to 100% correlation. Two models have been considered for zeolite L (LTL), assuming a pseudo-spherical $(2a = 9$ Å) and a pseudo-cylindrical $(2a = 9 \times 1.145 = 10.3$ Å) cage,
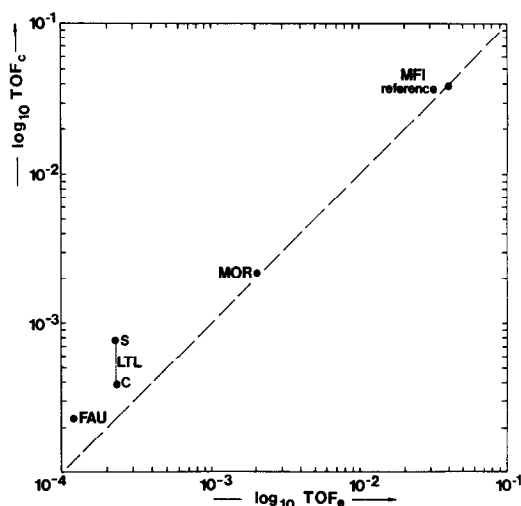

FIG. 6. Calculated (TOF_c) vs experimental (TOF_e) turnover frequency (rate in [mol (min cat–g)$^{-1}$/(Al/(Al + Si))] for MFI, MOR, LTL (spherical, S, and cylindrical, C, approximations), and FAU zeolites. Experimental data adapted from Ref. (49).

respectively. Excellent and unexpected agreement is observed, thereby supporting quantitatively the recent suggestion (2) that activity differences arise from nesting rather than from variations in acid strength. The slight deviation observed for FAU and LTL is the only indication for a possible effect of "site only" acid strength. It is a factor of about 2 and no more, far different from the two orders of magnitude variation in TOF which is observed experimentally.

This analysis demonstrates the need to consider structure-dependent contributions, such as physisorption effects (consistent with earlier views of Barrer (19)) which can act separately or in addition, and even dominate the effect of acid strength when sufficiently large molecules are considered. In the same vein, it may also help our rationalization of the difference in acid activity existing between amorphous and open framework crystalline aluminosilicates and provide a quantitative basis for the physical understanding of the recently proposed "energy gradient selectivity" (EGS) effect (59).

In addition, this approach shows that an

adequate definition and measure of acid strength should not be "static," i.e., involve local, electrostatic, or polarity factors only, such as those derived from infrared measurements. The ability of an acidic site to transfer a proton depends on several parameters: the polarity of the Brønsted hydroxyl group, the proton affinity of the accepting molecule, the capacity of the zeolite framework to accept and delocalize the residual negative charge, and the respective configurations and environment of the acid site and the reactant(s). Clearly, this situation is one where the *supermolecule concept* must be considered when catalytic activities must be rationalized. Note also that molecular nesting does not preclude the simultaneous occurrence of other shape selectivity effects.

Temperature Dependence of the Constraint Index

Recently, a dual mechanism for acid-catalyzed alkane cracking has been considered (*50*) to explain the temperature dependence (*51*) of the constraint index, $CI = k_H/k_P$, i.e., the ratio of cracking rate constants for *n*-hexane k_H and 3-methylpentane k_P. For ZSM-5, CI decreases with increasing temperature, from about 11 at 623 K to about 1.5 at 811 K. The proposed explanation is that a monomolecular reaction pathway, involving a less bulky transition state, is progressively favored as temperature increases (*50*). No allowance was made in this work for physisorption effects such as discussed above.

Assuming the dominance of the bimolecular mechanism of alkane cracking, and writing Eq. (15) for hexane (H) and 3-methylpentane (P), one obtains

$$k_H = k_{HT}(H) \cdot K_a(H) \qquad (20a)$$

$$k_P = k_{HT}(P) \cdot K_a(P) \qquad (20b)$$

and thus

$$CI = (k_H/k_P)$$
$$= A \cdot \exp[(\Delta Q_s - \Delta E)/RT] \qquad (21)$$

in which

$$\Delta E = E(H) - E(P) \quad \text{and}$$
$$\Delta Q_s = Q_s(H) - Q_s(P), \qquad (22)$$

ΔE being the difference in activation energy for the cracking of hexane relative to that of 3-methylpentane, and ΔQ_s representing the corresponding difference in physisorption heats. The entropy contribution is assumed to be identical for both reactions. A is then a parameter that is constant with respect to temperature. It follows that the variation of CI with temperature is expressed by the relation

$$\ln(CI_1/CI_2) = [(\Delta Q_s - \Delta E)/R]$$
$$\cdot [(T_2 - T_1)/T_1 \cdot T_2] \qquad (23)$$

which explicitly includes, via ΔQ_s, the effect of physisorption.

If physisorption effects are not considered and assuming no change in reaction mechanism, one concludes readily that CI should increase with temperature as hexane and 3-methylpentane crackings involve secondary and tertiary carbonium ions, respectively; i.e., the activation energy for hexane cracking should be higher than the corresponding value for 3-methylpentane ($\Delta E > 0$). The opposite variation is observed experimentally. This was at the origin of the dual-mechanism proposal which considers exclusively the effect of restricted transition state molecular shape selectivity (*50*).

However, assuming ΔE to be small (which is also implicit in the explanation proposed in Ref. (*50*)) relative to ΔQ_s, the temperature variation of CI can be estimated in two extreme cases considering ΔQ_s values ranging from 9.7 kJ mol^{-1} (obtained from Eq. (7a), setting the sorption energy of 3-methylpentane close to that of *n*-pentane) to about 49.1 kJ mol^{-1} (calculated from the high-temperature 513–553 K data of Table 1 in Ref. (*52*)). The computed ratio CI_{623}/CI_{811} is in the range 1.6–8.9 which compares rather well with the experimental observation, i.e., 7.3, and certainly

suggests that the effect of physisorption must be taken into account. It does not exclude per se that a monomolecular process can also take place, as proof for the latter was also based on the nature of the major saturated cracking products (50).

Nevertheless, variation of CI with temperature is definitely an observation which deserves further attention and needs to be extended to other zeolites. Measurements of sorption heats at temperatures close to reaction conditions would be extremely valuable for this purpose.

External Surface Molecular Shape Selectivity

Surface curvature effects are not restricted to the intracrystalline void volume of zeolites as their external surface also possesses catalytic activity varying with the amount of acidic sites associated with the presence of superficial structural aluminum (53). Depending on the zeolite nature, their hilly surface contains cut channels, pore openings, half-cavities, etc. where physisorption will be favored for molecules possessing adequate dimensions and conformations. Reactions occurring at such sites are likely to present some molecular shape-selective character and to show unexpected product selectivity.

Examples of these may already exist for the alkylation of aromatics over ZSM-5 catalysts (54–56), in particular the β-selective methylation of naphthalene (55, 56) or the synthesis of tridimensional chemicals (57). Such effects are likely to be enhanced for small (microcrystalline) zeolite catalysts and when access to the intracrystalline volume is restricted by either the pore size (small pore zeolites) or the feed molecule dimensions. Current work is in progress to probe these avenues.

CONCLUSIONS

Our primary conclusion is that active sites in zeolites and their direct environment constitute as a whole the entity responsible for the catalytic activity, a situation resembling that found in enzymes. *Zeolite-catalyzed reactions* must therefore be considered as *supermolecular conversions* because they also involve noncovalent interactions between the reactant(s) and the substrate. The concept described in this present paper is still in an embryonic stage although its foundation has been affirmed. It deserves and will receive further substantiation and consideration.

The consideration of *surface curvature effects* enables one to rationalize coherently various isolated observations in physisorption and catalysis by zeolites. Namely, the dependence of sorption heats on pore size is now accounted for in a continuous range of surface curvatures. An explanation is proposed for the several orders of magnitude difference between intracrystalline (self-)diffusion NMR coefficients and their Fickian macroscopic (uptake) analogs. The origin of the transport resistance on the surface of zeolite crystallites appears to lie, at least in part, in the need for a molecule sorbed on the external surface to "jump" over the convex pore rim into the concave channel or cavity. Two concepts which quantify earlier proposals have been introduced to describe diffusion in zeolites, i.e., the *floating* molecule which acquires supermobility when its dimensions match closely that of the surrounding channel and the molecular crawling or *creeping diffusion* along the channel walls for chain molecules.

Quantitative support for molecular *nesting* has been provided by derivation of the relation describing the dependence of cracking turnover frequency on effective pore size. Previous uncertainty about the relative importance of the roles played by acidity differences vs physical dimensions is now clarified, which may lead to a better definition of the acidic activity of zeolites in terms of the supermolecule concept. Surface curvature effects also explain successfully the dependence of the constraint index of ZSM-5 on temperature and the window

effect observed for the diffusion of C_3–C_{14} n-alkanes in erionite.

Evidence for external surface molecular shape selectivity should be sought. Using small crystallite size zeolites with pores too small to accept reactant molecules as catalysts is one possible step in this direction. Previous literature reports dealing with the conversion of bulky molecules on small and medium pore size materials should also be reevaluated in the light of the aforementioned proposals.

Current theoretical work is in progress to remedy the oversimplifications that make principally Eqs. (5a)–(5d) only semiquantitative, although they are convenient as rule of thumb for rapid estimates because they separate in factorized form the intrinsic molecular characteristics (polarizability, etc.) from the extrinsic geometrical effect associated with sorbent curvature. In particular, more realistic descriptions of the host–zeolite and guest–molecule polarizabilities are being introduced; new ways to simulate different channel networks are being designed; repulsion effects are being considered; long-range perturbations are better accounted for. Attention will also be paid to the nonequilibrium thermodynamic character of the processes that are involved.

ACKNOWLEDGMENTS

REFERENCES

1. Weisz, P. B., *I & EC Fundam.* **25**, 53 (1986).
2. Derouane, E. G., *J. Catal.* **100**, 541 (1986).
3. Fyfe, C. A., Kennedy, G. J., De Schutter, C. T., and Kokotailo, G. T., *J. Chem. Soc. Chem. Commun.*, 541 (1984).
4. Sirlin, C., *Bull. Soc. Chim. France*, 1–2, II-5 (1984).
5. de Laplace, P. S., "Mechanique Celeste," Supplement to Book 10, 1806.
6. For example, see Adamson, A. W., "Physical Chemistry of Surfaces," 3rd ed., p. 51. Wiley, New York, 1976.
7. Adamson, S. W., "Physical Chemistry of Surfaces," 3rd ed., p. 616. Wiley, New York, 1976.
8. Haag, W. O., Lago, R., and Weisz, P. B., *Faraday Discuss. Chem. Soc.* **72**, 317 (1981).
9. Kemball, C., *Adv. Catal.* **2**, 239 (1950).
10. Lucas, A. A., André, J. M., and Derouane, E. G., *Chem. Phys. Lett.* **137**(4), 336 (1987).
11. Schmeits, M., and Lucas, A. A., *J. Chem. Phys.* **65**, 2901 (1976).
12. Schmeits, M., and Lucas, A. A., *Surf. Sci.* **64**, 176 (1977).
13. Schmeits, M., and Lucas, A. A., *Prog. Surf. Sci.* **14**, 1 (1983).
14. Klinowski, J., Carpenter, T. A., and Gladden, L. F., *Zeolites* **7**, 73 (1987).
15. B. Nagy, J., Guelton, M., and Derouane, E. G., *J. Catal.* **55**, 43 (1978).
16. Steijns, M., and Froment, G. F., *I & EC Prod. Res. Dev.* **20**, 660 (1981).
17. Post, M. F. M., van Amstel, J., and Kouwenhoven, H. W., *in* "Proceedings, 6th International Zeolite Conference" (D. H. Olson and A. Bisio, Eds.), p. 517. Butterworths, Guildford, 1984.
18. Burch, R., and Warburton, C. I., *J. Catal.* **97**, 511 (1986).
19. Barrer, R. M., *in* "Zeolites: Science and Technology," NATO ASI Series E, No. 80, p. 227. Martinus Nijhoff, The Hague, 1984.
20. Derouane E. G., "Intercalation Chemistry" (S. Wittingham and A. J. Jacobson, Eds.), p. 101. Academic Press, New York, 1984.
21. Meier, W. R., and D. H. Olson, "Atlas of Zeolite Structure Types" Pub. Structure Commission of the Intern. Zeolite Assoc., 1978.
22. Stach, H., Lohse, U., Thamm, H., and Schirmer, W., *Zeolites* **6**, 74 (1986).
23. Rees, L. V. C., *Chem. Ind.* **7**, 252 (1984).
24. Nowak, A. K., and Cheetham, A. K., *in* "Proceedings, 7th International Zeolite Conference" (Y. Murakami, A. Iijima, and J. W. Ward, Eds.), p. 475. Kodansha–Elsevier, Tokyo, 1986.
25. Papp, H., Hinsen, W., Do, N. T., and Baerns, M., *Thermochim. Acta* **82**, 137 (1984).
26. de Boer, J. H., and Custers, J. F. H., *Z. Phys. Chem. B* **25**, 225 (1934).
27. Ruthven, A., *Amer. Chem. Soc. Symp. Ser.* **40**, 320 (1977).
28. Kärger, J. Bülow, M., Millward, G. R., and Thomas, J. M., *Zeolites* **6**, 146 (1986).
29. de Boer, J. H., *in* "The Dynamical Character of Adsorption," pp. 95–98. Oxford Univ. Press, London, 1953.
30. Barrer, R. M., *in* "Zeolites: Science and Technology," NATO ASI Series E, No. 80, p. 261. Martinus Nijhoff, The Hague, 1984.
31. Barrer, R. M., and Rosemblat, M. A., *in* "Proceedings, 6th International Zeolite Conference"

(D. H. Olson and A. Bisio, Eds.), p. 276. Butterworths, Guildford, 1984.

32. Barrer, R. M., and Davies, J. A., *Proc. R. Soc. London Ser. A* **322,** 1 (1971).
33. Barrer, R. M., "Symposium on the Characterization of Porous Solids, Neuchatel, 9–13th July, 1978."
34. Furuyama, S., Miyazaki, M., and Inoue, H., *J. Phys. Chem.* **88,** 1741 (1984).
35. Chen, N. Y., Lucki, S. J., and Mower, E. B., *J. Catal.* **13,** 329 (1969).
36. Gorring, R. L., *J. Catal.* **31,** 13 (1973).
37. Rabo, J., Bezman, R. D., and Poutsma, M. L., *Acta Phys. Chem. (Hung.)* **24,** 39 (1978).
38. Fraissard, J., Ito, T., Springuel-Huet, M., and Demarquay, J., *in* "Proceedings, 7th International Zeolite Conference" (Y. Murakami, A. Iijima, and J. W. Ward, Eds.), p. 393. Kodansha–Elsevier, Tokyo, 1986.
39. Mentzen, B. F., and Védrine, J. C., *C.R. Acad. Sci. Paris* **301**(II), 1017 (1985).
40. Derouane, E. G., and Hubert, R. J., *Chem. Phys. Lett.* **132,** 315 (1986).
41. Derouane, E. G., and Fripiat, J. G., *Zeolites* **5,** 165 (1985).
42. Derouane, E. G., Baltusis, L., Dessau, R. M., and Schmitt, K. D., *in* "Catalysis by Acids and Bases" (B. Imelik *et al.,* Eds.), *Stud. Surf. Sci. Catal.,* Vol. 20, p. 135. Elsevier, Amsterdam, 1985.
43. Barthomeuf, D., *J. Phys. Chem.* **83,** 249 (1979).
44. Mortier, W. J., *J. Catal.* **55,** 138 (1978).
45. Jacobs, P. A., *Catal. Rev. Sci. Eng.* **24,** 415 (1982).
46. Sohn, J. R., DeCanio, S. J., Fritz, P. O., and Lunsford, J. H., *J. Phys. Chem.* **90,** 4847 (1986).
47. Freude, D., Hunger, M., and Pfeifer, H., *Chem. Phys. Lett.* **128,** 62 (1986).
48. Fukase, S., and Wojciechowski, B. W., *J. Catal.* **102,** 452(1986).
49. Kikuchi, E., Nakano, H., Shimomura, K., and Morita, Y., *Sekiyu Gakkaishi* **28,** 210 (1985).
50. Haag, W. O., and Dessau, R. M., *in* "Proceedings, 8th International Congress on Catalysis, Berlin, 1984," p. II–305. Verlag Chemie, Weinheim, 1985.
51. Frilette, V. J., Haag, W. O., and Lago, R. M., *J. Catal.* **67,** 218 (1981).
52. Santilli, D. S., *J. Catal.* **99,** 335(1986).
53. Gilson, J. P., and Derouane, E. G., *J. Catal.* **88,** 538 (1984).
54. Ducarme, V., and Védrine, J. C., *Appl. Catal.* **17,** 175 (1985).
55. Fraenkel, D., Cherniavsky, M., and Levy, M., *in* "Proceedings, 8th International Congress on Catalysis, Berlin, 1984," p. IV–545. Verlag Chemie, Weinheim, 1985.
56. Fraenkel, D., Cherniavsky, M., Ittah, B., and Levy, M., *J. Catal.* **101,** 273 (1986).
57. Jacobs, P. A., Tielen, M., and Sosa, R. C., *in* "Structure and Reactivity of Modified Zeolites" (P. A. Jacobs *et al.,* Eds.), *Stud. Surf. Sci. Catal.,* Vol. 18, p. 175. Elsevier, Amsterdam, 1984.
58. Fraissard, J., *in* "Catalysis by Zeolites" (B. Imelik *et al.,* Eds.), *Stud. Surf. Sci. Catal.,* Vol. 5, p. 343. Elsevier, Amsterdam, 1980.
59. Mirodatos, C., and Barthomeuf, D., *J. Catal.* **93,** 246 (1985).
60. Barrer, R. M., *in* "Zeolites and Clay Minerals as Sorbents and Molecular Sieves," p. 194. Academic Press, London, 1978.